ADVANCED MATERIALS

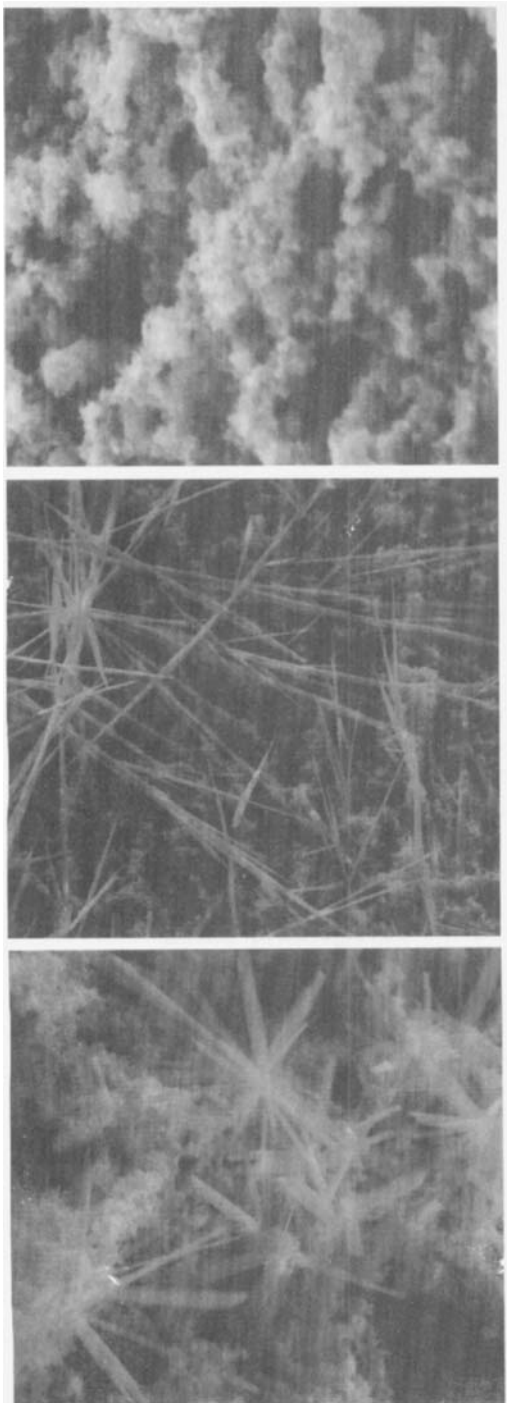

Fig. 3. SEM pictures. Top) Film as formed electrochemically (13 mm represents 10 μm). Middle and Bottom) After 24 h with intermittent polarization to 0.5 V (middle: 30 mm represents 100 μm; bottom: 10.5 mm represents 10 μm).

polymerization occurring when a potential is applied to the electrode. The polymerization process is fast and may favor a spherical growth of the chains.

*Experimental*

The solution used for the electrosynthesis had the composition: 1 M $H_2SO_4$, 0.5 M $Na_2SO_4$, 0.1 M 2,5-dimethoxyaniline and 5 mM aniline. Addition of the latter monomer was necessary to avoid shedding of the polymer film after several hours. The polymerization was carried out using cyclic voltammetry, at the scan rate of 50 mV/sec, between −0.2 and 0.65 V. 50 cycles were always run and the final voltage was −0.2 V, resulting in fully reduced PDMA. The working electrode was a Pt foil of 0.56 $cm^2$ framed by Teflon ribbon, while SCE was used as a reference electrode. $N_2$ was bubbled through the solution for a considerable time before starting the experiments and the cells were kept tightly closed thereafter, so that the $O_2$ content was reduced to negligible values. Thus, an $O_2$ influence on the post-polymerization events can be ruled out. The experiments were driven by a PAR 273 potentiostat interfaced with a computer. The latter allowed the calculation of the charge associated with each half-cycle.

Received: August 27, 1993
Final version: October 7, 1993

[1] M. Pasquali, G. Pistoia, R. Rosati, *Synth. Met.* **1993**, *58*, 1.
[2] G. Pistoia, R. Rosati, *Electrochim. Acta*, in press.
[3] G. Zotti, N. Comisso, G. D'Aprano, M. Leclerc, *Adv. Mater.* **1992**, *4*, 749.
[4] G. D'Aprano, M. Leclerc, G. Zotti, *J. Electroanal. Chem.* **1993**, *351*, 145.
[5] E. M. Genies, M. Lapkowski, *J. Electroanal. Chem.* **1987**, *236*, 199.
[6] S. H. Glarum, J. H. Marshall, *J. Electrochem. Soc.* **1987**, *134*, 2160.

## Absolute Calibration of Microwave Loss in ESR Spectrometers

By *Sivert H. Glarum, Arthur P. Ramirez,* and *Robert C. Haddon**

With the advent of high-$T_c$, organic and $C_{60}$ superconductors has come the realization that studies of field-dependent microwave loss offer several unique advantages for the detection and characterization of superconducting materials.[1 - 11] The measurements themselves are made with conventional electron spin resonance (ESR) spectrometers. Data interpretations, however, are generally qualitative and, as the loss mechanisms are moot and probably of varied origins, a quantitative technique relating measured voltages to energy dissipation in a sample would be helpful in unraveling material behavior. An absolute calibration procedure, accurate to ≈5% has been developed demanding only a frequency counter, a DC voltmeter, and a ball bearing. As this problem is equivalent to finding the number of spins in a paramagnetic sample by ESR, or more correctly a magnetic susceptibility contribution, the procedure may also be of interest to those engaged in conventional ESR spectroscopy. Despite the simplicity of the technique, a literature search has failed to reveal an awareness of the basic method, conventional spin-counting methods largely relying on comparisons with reference paramagnetic spectra. Apart from the advantages offered by a completely electrical calibration procedure, this method may be useful in situations, e. g. low temperature, where reliable standards are lacking.

Although most ESR spectrometer configurations exhibit considerable customized variabilities, a brief description of ours will be helpful in clarifying the calibration procedure.

[*] Dr. R. C. Haddon, Dr. S. H. Glarum, Dr. A. P. Ramirez
AT & T Bell Laboratories
Murray Hill, NJ 07974 (USA)

  *0935-9648/94/0101-059 $ 5.00+.25/0* 

The microwave "bridge" is based on a gyrator with the three ports connected to a klystron source, the cavity, and a detector. The klystron is controlled by a Varian V4500-10A unit with 40 kHz automatic frequency control (AFC) circuitry. The cavity arm terminates in an iris-coupled Varian V4531 $TE_{102}$ cavity containing an APD LTR helium dewar insert and this arm also includes a slide-screw tuner to provide a homodyne reference for detector biasing. As a detector, we are using an MA40194 diode whose output is connected in parallel to the AFC controller and a PAR 5210 lock-in amplifier. For reasons to become evident, it was necessary to install an alternative, switch-selected AFC input circuit flat in frequency response from DC to 2 kHz (the normal configuration, with its coupling transformer, milliammeter, and electrolytic capacitor, shows substantial impedance changes below 20 Hz). The lock-in unit also provides the field modulation source which, with a power amplifier, drives the modulation coils at frequencies up to 100 kHz.

For a variety of reasons, and in particular field-modulation calibrations, it is desirable to have a paramagnetic reference with a strong, narrow, Lorentzian, absorption. The only materials we have found adequate are sugar chars, and their preparation may be of general interest. A canonical teaspoon of sucrose is heated in a beaker on a hotplate for several hours until reduced to a solid black mass showing no tackiness. This residue is then transferred to an open tube and heated in a 450 °C furnace for 1 h to drive out trace residual volatiles. A small quantity, <1 mg, is placed in a 1 mm quartz capillary, evacuated to <1 μm, and sealed off. The capillary is then put in a 625 °C furnace. At this temperature an intense paramagnetism quickly develops, $\approx 10^{17}$ spins/mg, and its width may be controlled by the time in the furnace—5 min, 2 G; 10 min, 1 G; 20 min, 0.5 G. This temperature is rather critical, if too low, signal growth is slow, if too high, the radicals disappear. Comparisons of the amplitudes of derivative ESR spectra with their first and second integrals give ratios within 1% of those for theoretical Lorentzian shapes after truncation corrections.[12] Thus, such samples may be used for field-modulation calibrations using Wahlquist's analytical expressions.[13] It should be noted that these samples saturate at power levels >10 mW.

Formally, the voltage measured by the lock-in, $V_m$, is related to the cavity reflection coefficient, $\varrho$, by Equation 1.

$$\Delta V_m = (dV_m/d|V|)_{op}|V^+ \Delta\varrho| \quad (1)$$

$|V|$ is the effective microwave voltage incident upon the detector and $|V^+|$ that incident upon the cavity. The derivative coefficient depends on diode parameters, a frequency-dependent load impedance, and the bias level at the operation point (op), while $V^+$ varies with the power level. The cavity reflection coefficient is given by

$$\varrho = (Z - Z_0)/(Z + Z_0) \quad (2)$$

with

$$Z/Z_0 = iQ_0[1 - (\omega_0/\omega)^2] + Q_0/Q \quad (3)$$

$\omega_0$ is the cavity's resonant frequency, $Q$ the cavity $Q$ value, and $Q_0$ a parameter dependent on waveguide impedance and iris coupling. At resonance and critical coupling, $\varrho = 0$ and $Q_0 = Q$. Consider a situation with the iris adjusted for critical coupling and the frequency shifted from resonance by varying the klystron's reflector voltage with AFC disabled until the detector reaches its standard bias level. We now vary the frequency about this point, measuring the DC level at the detector as a function of frequency,

$$\Delta V_m/\Delta\omega = (dV_m/d|V|)_{op}|V^+|(\Delta|\varrho|/\Delta\omega) \quad (4)$$

and, from Equations 2 and 3,

$$\Delta|\varrho|/\Delta\omega = (Q/\omega)(1 - |\varrho|^2)^{3/2} \quad (5)$$

This measurement is expedited by a simple computer program which alternately measures frequency and voltage until consecutive readings agree and then calculates a linear least-squares value for $\Delta V_m/\Delta\omega$ when 20–30 points have been accumulated. For a nominal 1 mW microwave power level, we typically find results of order $0.2 \pm 0.0005$ V/MHz, with the standard deviation for measurements spanning a 2:1 potential range given by Birge's formula.[14] Repeated measurements, however, at different times or bias conditions show 2% reproducibilities.

The factor involving $\varrho$ in Equation 5 is a minor correction. When the tuner has been adjusted for a normal bias level, $|\varrho|$ may be estimated from the mode sweep pattern by noting the change in attenuator setting required to raise the cavity dip minimum to the level of the mode sweep maxima. The reflection coefficient is then the ratio of ESR spectrum amplitudes measured at these two settings. At 1 mW, we find $|\varrho| \sim 0.2$, giving a 6% correction.

A more serious correction stems from the frequency-dependence of $dV_m/d|V|$. The above procedure yields the DC value and it is necessary to determine corrections for specific modulation frequencies, thus the necessity for a detector circuit with a flat frequency response from DC to a frequency convenient for measuring ESR spectra. Comparison of the amplitudes of a spectrum measured with a 'flat' circuit at low frequencies with one made at the desired frequency using the normal detector circuitry then gives the approprite correction factor. For our spectrometer this is a factor of 3, but the relative amplitudes can be rather accurately determined (<1%) if modulation fields are properly calibrated and levels used for which the signal is a maximum. Combining Equations 1, 4 and 5 gives Equation 6 with the subscript c denoting corrections for frequency and finite $\varrho$.

$$\Delta V_m = (dV_m/d\omega)_c\,(\omega/Q)|\Delta\varrho| \quad (6)$$

A more elegant procedure, but one involving more sophisticated instrumentation, is to frequency modulate the mi-



0935-9648/94/0101-060 $ 5.00+.25/0 Adv. Mater. 1994, 6, No. 1

ADVANCED MATERIALS

crowave source at a calibrated level at the desired frequency and measure the detector signal at this frequency deviation from cavity resonance. Qualitatively, this information is present in the AFC error signal, and monitoring this signal for a fixed modulation index may be used to account for routine variations of power level and cavity $Q$ without recourse to recalibration.

$$\Delta Q = (Q/2)\Delta(1/Q) \tag{7}$$

For a critically coupled cavity at resonance, Equations 2 and 3 give Equation 7 with the change in $Q$ due to absorption processes. As defined, $\omega/Q$ is the ratio of power dissipated to the maximum energy stored in magnetic fields within the cavity (this is equivalent to the ratio $R/L$ when the cavity is represented by a lumped series $LCR$ circuit element). Thus Equation 8 holds with $P$ the power in erg/s, $H$ the peak temporal microwave field in gauss, and the integration over the cavity volume in $cm^3$.

$$\omega\Delta(1/Q) = \Delta P/[(1/8\pi)\int H^2\,d\tau] \tag{8}$$

The second stage of calibration makes use of cavity perturbation theory. As shown by Maier and Slater,[15] insertion of a small metallic sphere in a cavity at an E-field node gives a frequency shift (Eq. 9) where $v$ is the volume of the sphere and $H_s$ the peak microwave field at the sphere's position.

$$\Delta\omega/\Delta v = (3/4)\omega H_s^2/\int H^2\,d\tau \tag{9}$$

Using a set of five 1/16″ precision ball bearings we measure a value of 1883 $\pm$6 MHz/$cm^3$. The theoretical value for an empty $TE_{102}$ cavity of similar dimensions is 1300, and we see the field enhancement due to cavity loading by the quartzware. Combining Equations 6–9 yields Equation 10.

$$\Delta V_m = (16\pi/3)(dV_m/d\omega)_c(\Delta\omega/\Delta v)(\Delta P/\omega H_s^2) \tag{10}$$

The novel aspect of this result is that it directly yields the ratio of energy dissipated to $H_s^2$, the parameter actually desired in measurements of linear dissipative phenomena, without the need to know power levels, cavity $Q$s, or actual field intensities. For a magnetic resonance Equations 11 and 12 hold where $\Delta H_m$ is the magnetic field modulation.

$$P = (1/2)\omega\chi'' H_s^2 \tag{11}$$

$$\Delta V_m = (8\pi/3)(dV_m/d\omega)_c(\Delta\omega/\Delta v)(d\chi''/dH)\Delta H_m \tag{12}$$

$$\int\chi''dH = (1/2)\pi H_0\chi_0 \tag{13}$$

On the basis of Equation 13, double integration of an experimental spectrum suffices for calculating the contribution to the static susceptibility of an absorption centered at $H_0$. For a system of uncoupled spins Equation 14 holds, the latter numerical coefficient applying for $g = 2$, $S = 1/2$, and $T = 293$ K.

$$\chi_0 = (N/3kT)\,g^2\beta^2 S\,(S+1) = 1.28\times10^{-3}\,N/N_{av} \tag{14}$$

To test this calibration scheme, we measured the ESR spectra for two samples each of three different paramagnetic solids, and results are summarized in Table 1. The determined values for $\chi_0$, obtained from doubly integrated spectra, range within ~10% of their correct values, but it is evident that a major error lies in accurately weighing the small quanities of material. The spectra are rather different in character. That of the $Cu^{2\oplus}$ salt is highly anisotropic and a finely ground sample had to be used. The spectrum of the $Mn^{2\oplus}$ salt ($S = 5/2$) has a 195 $G_{pp}$ Lorentzian shape and a 19% correction was made to account for truncation by the 2500G sweep used.[12] The nitroxide has a much narrower spectrum, ~12 G, but is clearly inhomogeneous.

Table 1. Molar magnetic susceptibilities calculated from ESR spectra.

| | $\chi_0$ [$\times 10^6$ $cm^3$] (lit.) | [mg] | $\chi_0$ [$\times 10^6$ $cm^3$] (meas.) | ratio |
|---|---|---|---|---|
| $CuSO_4 \cdot 5H_2O$ | 1460 [a] | $2.5_0$ | 1450 | 1.00 |
| | | $3.5_6$ | 1650 | 1.13 |
| $MnSO_4 \cdot H_2O$ | 14200 [a] | $1.9_6$ | 15260 | 1.07 |
| | | $6.3_1$ | 14020 | 0.99 |
| 4-hydroxy-TEMPO [c] | 1256 [b] | $1.1_3$ | 1300 | 1.04 |
| | | $2.1_3$ | 1110 | 0.88 |

[a] *Handbook of Chemistry and Physics*, 54th ed., CRC Press, **1973**. [b] A. Blaise et al., *C.R. Acad. Sci.* **1972**, *274B*, 157. [c] TEMPO = 2,2,6,6-tetramethylpiperidinyloxy.

Table 1 reveals no systematic errors in the calibration, suggesting that corrections have been taken into account at the 5% level. Based on the reproducibility of the various measurements going into the calibration coefficient, the principal error lies in determining $(dV_m/d\omega)$, ~2%, with other factors reproducible to $\leq$1%. The lock-in amplifier range calibrations are specified accurate to 3% for bandpass operation, and so an estimated accuracy of 5% is in accord with both expectation and observation.

Although the method is reported here in full detail for the first time, it has previously found extensive use in our laboratory for the measurement of magnetic susceptibilities[16,17] and the characterization of superconductors.[1,6,17] This technique provided the first indication of superconductivity in K- and Rb-doped $C_{60}$.[8–10]

In summary, we have described a calibration procedure for ESR spectrometers which allows a quantitative interpretation of measured voltages in terms of magnetic losses, $\chi''$, with ~5% accuracy. This procedure makes no use of paramagnetic reference materials. It is wholly electrical, requires only a microwave frequency counter and a DC voltmeter, and circumvents the need to be able to determine cavity $Q$s, power levels, or field strengths. Given a relationship between

  *0935-9648/94/0101-061 $ 5.00+.25/0* 

$\chi_0$ and the number of spins in a material, one can then determine the latter with equivalent accuracy.

Received: August 19, 1993
Final version: October 11, 1993

[1] S. H. Glarum, J. H. Marshall, L. F. Schneemeyer, *Phys. Rev. B* **1988**, *37*, 7491.
[2] R. Durny, J. Hautala, S. Ducharme, B. Lee, O. G. Symko, P. C. Taylor, D. J. Zheng, *Phys. Rev. B* **1987**, *36*, 2361.
[3] K. W. Blazey, K. A. Muller, J. G. Bednorz, W. Berlinger, G. Amoretti, E. Buluggiu, A. Vera, F. C. Matacotta, *Phys. Rev. B* **1987**, *36*, 7241.
[4] B. F. Kim, J. Bohandy, K. Moorjani, F. J. Adrian, *J. Appl. Phys.* **1988**, *63*, 2029.
[5] A. Dulcik, R. H. Crepeau, J. H. Freed, *Phys. Rev. B* **1988**, *38*, 5002.
[6] R. C. Haddon, S. H. Glarum, S. V. Chichester, A. P. Ramirez, N. M. Zimmerman, *Phys. Rev. B* **1991**, *43*, 2642.
[7] J. Bohandy, B. F. Kim, F. J. Adrain, K. Moorjani, S. D'Arcangelis, D. O. Cowan, *Phys. Rev. B* **1991**, *43*, 3724.
[8] S. H. Glarum, S. J. Duclos, R. C. Haddon, *J. Am. Chem. Soc.* **1992**, *114*, 1996.
[9] A. F. Hebard, M. J. Rosseinsky, R. C. Haddon, D. W. Murphy, S. H. Glarum, T. T. M. Palstra, A. P. Ramirez, A. R. Kortan, *Nature* **1991**, *350*, 320.
[10] M. J. Rosseinsky, A. P. Ramirez, S. H. Glarum, D. W. Murphy, R. C. Haddon, A. F. Hebard, T. T. M. Palstra, A. R. Kortan, S. M. Zuharak, A. V. Makhija, *Phys. Rev. Lett.* **1991**, *66*, 2830.
[11] R. C. Haddon, *Acc. Chem. Res.* **1992**, *25*, 127.
[12] I. B. Goldberg, *J. Magn. Res.* **1978**, *32*, 233.
[13] H. Wahlquist, *J. Chem. Phys.* **1961**, *35*, 1708.
[14] R. T. Birge, *Phys. Rev.* **1932**, *40*, 207.
[15] L. C. Maier, Jr., J. C. Slater, *J. Appl. Phys.* **1952**, *23*, 68.
[16] M. P. Andrews, A. W. Cordes, D. C. Douglass, R. M. Fleming, S. H. Glarum, R. C. Haddon, P. Marsh, R. T. Oakley, T. T. M. Palstra, L. F. Schneemeyer, G. W. Trucks, R. Tycko, J. V. Wasczak, K. M. Young, N. M. Zimmerman, *J. Am. Chem. Soc.* **1991**, *113*, 3559.
[17] R. C. Haddon, A. P. Ramirez, S. H. Glarum, unpublished.

## Monocrystalline $Si_3N_4$ Filaments

By *Klaus J. Hüttinger** and *Torsten W. Pieschnick*

Advanced monolithic ceramics for applications as structural materials at very high temperatures still exhibit decisive disadvantages, namely high-temperature creep and low damage tolerance. Reinforcement fibers for the synthesis of ceramic matrix composites, which are more promising for such applications, are of limited usefulness: a) Carbon fibers are stable at high temperature, but readily undergo oxidation above 500 °C. Therefore, the problem is shifted to complex oxidation protection systems. b) Ceramic fibers based on silicon carbide, alumina or mullite have limited high-temperature stability for various reasons, i.e. recrystallization and reactions between the phases of the non-stoichiometric fiber materials. c) Whiskers are mono-crystalline, and thus stable, but problems arise from their geometry.[1, 2]

For the production of high-temperature stable ceramic fibers, the polymer precursor route seems to be the most attractive for future development but much work still remains to be done. As an alternative and less complex route, the synthesis of monocrystalline silicon nitride filaments was investigated.[3] The design considerations of such a synthesis led to a catalyzed chemical vapor deposition process. Such a process is based on adsorption and dissociation of volatile compounds at the catalyst surface, dissolution of the elements forming the desired compound and precipitation of this compound.

As nitrogen sources molecular nitrogen and ammonia were selected. Silicon hydrides instead of silicon chlorides were employed as silicon sources for environmental reasons. To avoid expensive monosilane, $SiH_4$, silicon subhydrides, $SiH_x$ ($x = 1,2$) were produced in situ by reaction of silicon powder (technical grade) with hydrogen at 1300 °C. Since silicon particles show a high tendency to sinter under such conditions the particles were pretreated with nitrogen at 1150 °C to form a thin layer of silicon nitride. This layer proved to be very effective. Constant $SiH_x$ formation rates up to nearly 50% silicon conversion could be achieved.

For the selection of the catalyst material the following criteria were assumed to be decisive: Solubility of silicon and nitrogen, but no formation of a stable nitride. Iron seemed and proved to fulfil these requirements. A suitable substrate material for the iron particles (fractions from 1 to 3 and 5 to 8 μm in diameter) should neither be attacked by the gas phase nor wetted by the catalyst particles. Alumina was tested as an insulator as it cannot form selective electron–electron interactions with a metal, and found to be applicable. Non-wetting of the substrate by the catalyst is an absolute necessity for the filament growth, which only occurs if the catalyst particle is located at the tip of the growing filament.

$$Si + H_2 \xrightarrow[1300\,^\circ C]{} SiH_x + N_2/NH_3 \xrightarrow[1300\,^\circ C]{Fe[Al_2O_3]} Si_3N_4 + H_2 \quad (1)$$

Conclusively, the reaction sequence shown in Equation 1 was investigated. Experimental studies were performed at 1300 °C and various flow rates of $N_2$, $N_2/NH_3$ and $SiH_x/H_2$ mixtures using the reactor shown in Figure 1. Silicon nitride

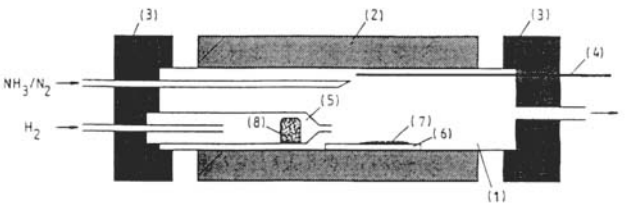


Fig. 1. Diagram of the experimental reactor; (1) reactor tube, (2) furnace, (3) water cooled flanges, (4) thermocouple, (5) internal reactor tube for $SiH_x$ production, (6) substrate (alumina), (7) catalyst particle, (8) silicon powder.

filaments were obtained only with ammonia. This result can be explained by two effects: a) The low adsorption probability of nitrogen as compared to ammonia at an iron surface, which is about 6 orders of magnitude lower.[4] b) The high difference of the bond dissociation energies of $N_2$ and $NH_3$:

[*] Prof. K. J. Hüttinger, Dr. T. W. Pieschnick
Institut für Chemische Technik der Universität Karlsruhe
Kaiserstrasse 12, D-76128 Karlsruhe (FRG)



0935-9648/94/0101-062 $ 5.00+.25/0